Response to Reviewers

We thank the two reviewers for their comments on the manuscript. We have responded to every reviewer comment (highlighted in italics).

General comment

The introduction does not adequately pose the scientific question nor state the importance of this research. (Reviewer #1)

We have revised the introduction to improve the description of the paper, including in particular some of the summary comments from the last section to emphasise the purpose of the age of air section of the paper. The introduction now addresses the next point made by the reviewer.

Why is it important to calculate the actual age of the emissions as opposed to the photochemical age? (Reviewer #1)

The main objective of the age of air calculation is to quantify the effects of photochemical retardation due to aerosols within a biomass burning plume. Quantifying the retardation is achieved by computing the physical and photochemical age of the plume. We have clarified this point in the introduction.

Referee #1

You should discuss the results of Parrington et al (2012, 2013) including limitations of the methods employed …and the benefits of the new method

Limitations of the photochemical age method are briefly discussed in regards to OH assumptions in line 7 page 8735. We have extended this section to include other limitations of this method and therefore the results in Parrington et al 2013. We have also included the advantages of our new method.

Wouldn't it make more sense to use a finer spatial resolution in the model?

To address this reviewer response we have run the model at other spatial resolutions, including nested model simulation over the BORTAS study region at a resolution of 0.5° latitude and 0.667° longitude during July 2011. As discussed below, this provides a more difficult test for the emission inventories.

Can you speculate on the impact to your conclusions?

We have now run the model at higher spatial resolutions and driven it using different emission inventories for biomass burning to assess uncertainties introduced by emissions and atmospheric transport. In summary using the nested resolution does not change the outcome the results of the paper although they do highlight the incorrect spatial distribution of CO emissions from biomass burning that was less obvious using the coarse resolution. We have changed the manuscript to include these points as described in more detail below.

We have run GEOS-Chem at 2° latitude and 2.5° longitude using FLAMBE biomass burning emissions to test the transport in the model. Emissions of CO from FLAMBE appear to be broadly qualitatively consistent with GFED3 emissions. The model shows similar skill in capturing the variability of the biomass burning plumes with both emission inventories but FLAMBE has a larger positive bias particularly within air masses identified as biomass burning plumes. This bias might also be due to errors in atmospheric transport at high altitudes. The GEOS-Chem model distributes the GFED3 biomass burning emissions evenly though the boundary layer, without consideration of injection heights above the boundary layer which would subsequently affect transport of emitted CO (see below).

We have also run the tagged CO model using the native-resolution nested grid over North America for July 2011 to cover the BORTAS period. The nested model has similar skill to the coarser

resolution in reproducing all the BORTAS aircraft data (Pearson r^2 = 0.28). We find that the model has better skill at reproducing results at lower levels below 4 km (r^2 = 0.36) compared to higher altitudes (r^2 = 0.02). In the revised paper we argue that the Spearman's rank correlation is the more appropriate metric, reflecting our ability to identify plumes but not necessary reproduce the elevated values. We find that Spearman's rank correlation is 0.65 below 4 km and 0.19 above 4 km.

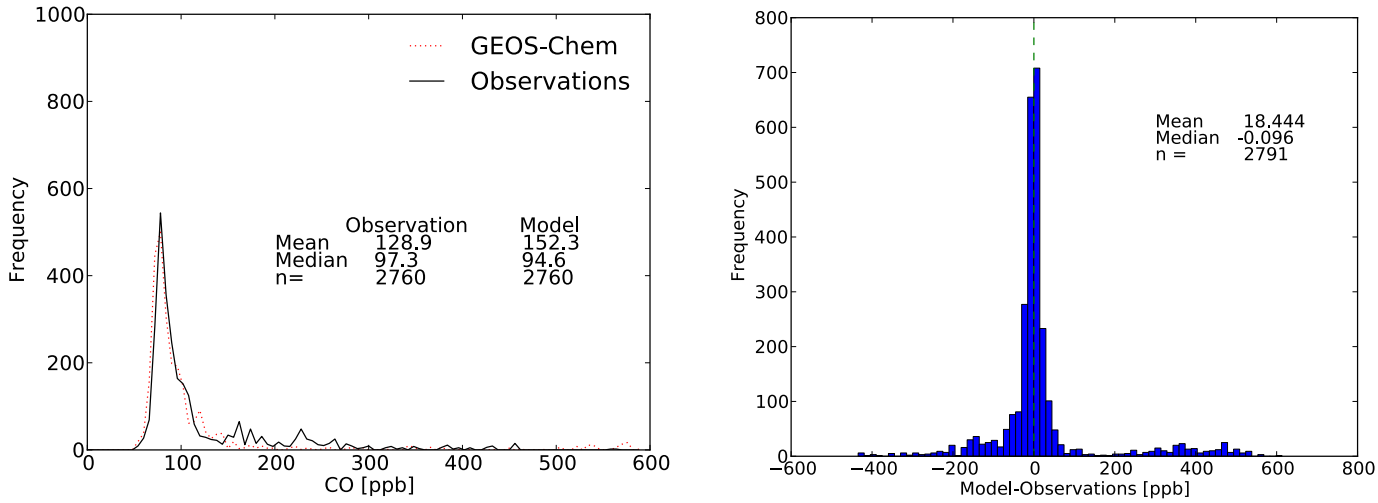

Figure 1 Statistical comparison of model and observed CO from BORTAS-B for the nested grid. The observations have been averaged over the 0.5 x 0.667 degree model grid. Left panel shows the frequency distributions and the right panel shows the frequency distribution of the model minus observed CO residuals. Mean and median values are shown inset of each panel.

We find that the nested model overestimates the CO in the plumes up to a factor of 5. This large discrepancy is due to overestimating CO emissions from the GFED3 emissions dataset. In the coarser model run, the high CO values on a fire hotspot are reduced, as expect, because of spatial averaging of small-scale features. The mean residual CO is 18.4 ppb with a standard deviation of 132.3 ppb and a median of -0.1 ppb.

Figure 2 shows the vertical resolution of this bias according to pressure bins. The largest discrepancy is between 750 and 850 hPa with a mean proportional difference of 2. There is a small positive model bias between the surface and 900 hPa and a small negative bias above 750 hPa. This strengthens the hypothesis that the model does not distribute CO emissions well.

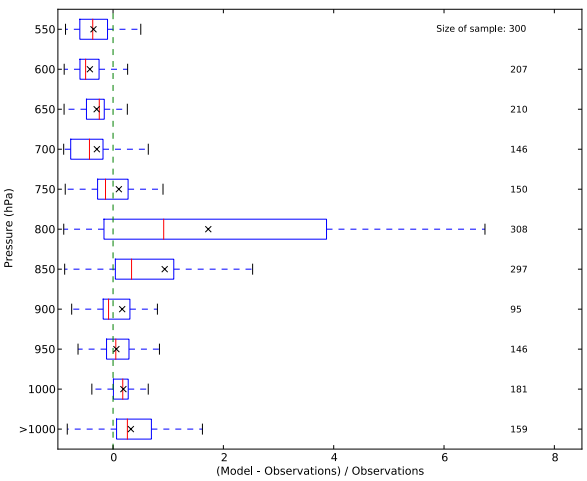

Figure 2 Relative model error in the GEOS-Chem simulation of CO during BORTAS-B as a function of altitude described by the box and whiskers approach. The red line and grey cross denotes the median and mean values, respectively.

I would like to see some actual data-model comparisons along the flight tracks

Figure 3 shows observed and model CO concentration along all the flight tracks combined for the nested resolution. The model reproduces background CO but do not reproduce the very highest values of CO associated with biomass burning. This bias is more prominent at the higher resolution, supporting our hypothesis that the distribution of CO emissions in the model is wrong. We have left this figure out of the manuscript because it does not add anything to the readability of the paper, especially given the additional text added as part of the revision (see above).

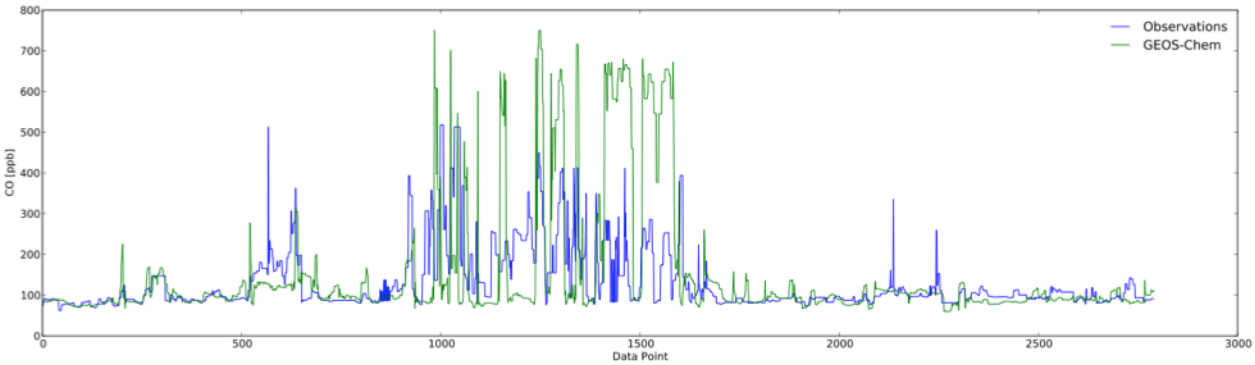

Figure 3 CO concentrations along all the flight paths during BORTAS-B from GEOS-Chem (green) and observations (blue).

It seems as if you are saying that even though your model has very little skill (r2 = 0.2) at reproducing individual observations, I should believe your conclusions because your median and mean are similar. I recommend you provide a more convincing justification.

This a fair point. See above response related to our revised calculations.

In short, using the higher resolution model for the age of air analysis strengthens our results. We now show the r-squared value of 'difference between photochemical and physical effective age' and 'effective age' to have risen from 0.60 to 0.80 inside the plume but only risen from 0.23 to 0.28 outside the plume. This strengthens our claim that the major reason for the difference in the two age measures is due air being within a BB plume or not (and therefore the levels of OH, most likely controlled by aerosol concentration). The age of air calculation will be affected by the incorrect spatial distribution of the CO, but not by the inconsistencies with the amount of emissions as the calculation does not take into account the size of the CO emissions. The updated plots will be included in the manuscript.

Referee #2

Consistency in referring to it as 'physical' or 'effective' would help

We thank the reviewer for raising this point. To clarify this point we have consistently renamed this metric the effective physical age or $\bar{A}$.

What effect would having a lower OH value have on your conclusions? Is it sensitive to OH?

All EPA values we report in our domain are well below the e-folding lifetime set by OH therefore diffusion is the dominant effect. We have run the analysis with a doubled and halved lifetime and the ages differ by less than one day. As stated in the paper (page 8735, line 13 -14), halving (doubling) the OH concentration would double (halve) the photochemical lifetime, but this was chosen by Parrington et al 2013 to reflect the photochemical environmental at that latitude and season.

If "correct" OH were used, would the effective age match the photochemical age? Is this a way of deducing mean OH?

We see your argument. The "correct" OH would be OH sampled along the flight track for the age of air calculation. The photochemical age calculation uses only one value of OH, representative of the background atmosphere, to underpin the whole calculation. The difference between the physical and photochemical ages would then provide information about the integrated OH concentration along the flight track, assuming that atmospheric diffusion played no role in mixing the air. We think the compounded errors associated with every stage of such a calculation would preclude a reliable estimate for mean OH.

*A brief description of how photochemical age was calculated would hel*p

In the interest of brevity we referred to the Parrington et al 2013 paper in our previous manuscript. However, we now nclude a brief description for readers as well as references with more a more detailed description of how photochemical age is calculated.

Contradictory *terms in abstract, p 8728 and 8733*

Thank you for pointing these out. This has been corrected.

Line 15 - 16: How can a median be a range?

This has now been changed to "median difference… 3 days" - This has also been updated to match the new higher resolution model run on the advice of reviewer #1

Page 8729 line 3: Most frequent is the mode.. why is it a range and not a single number?

This has been amended to the following statement: " The interquartile range for observed CO is 87--126 ppb with a mode of 90 ppb. This is consistent with background CO measurements during the NASA ARCTAS-B campaign…"

Page 8730 line 12: Should be "are due" not "is due"

This has been changed in the revised manuscript.

Page 8731 Line 11: add W after 50 degree

This has now been amended. We have also amended the definition of the latitude averaging area to the correct co-ordinates (45 - 60 degrees north) to match the figure.

Line 15 onwards: confusing section. … did not get the same numbers… some ambiguity in which numbers specifically you are referring to … suggest editing this section to make it clear and unambiguous

We have reworded the paragraph to make it clearer. The changes are stated below.

- (Line 15 - end of line 18) "At the western boundary, emission from 2008 have a median age of 7 days, 2009 has a median age of 10 days and 2010 and 2011 have a median age of 5 days. The age of air at the western boundary in 2009 has a larger age range than the other years with generally older air (from 2 to 20 days). We find the older age of emissions during 2009 is due to fewer fires along the western boundary so that sampled air originates from Alaska and further upwind."

- (Line 21 - line 22) "The eastern boundary for all years and at all altitudes have median values between 11 and 13 days and a range of 2 - 23 days."

- (Line 24 - line 28) “The age of emissions clearly gets older moving towards the Atlantic, consistent with westerly flow, with an increase in median age of approximately 3 days for all years except 2009, where the age difference between the west and east boundary is approximately one day in the lower troposphere and no differences for higher altitudes. We attribute the lack of ageing in 2009 to the less fresh emissions in Canada during July of this year. Boreal biomass burning in 2009 was seen earlier in the season and was more prominent in Alaska and Siberia.”

Page 8732 Line 10: give co-ordinates for Thunder Bay

We have added coordinates for Thunder Bay.

Page 8732 Line 11: *Does 16-17 July equate to 3-4 contour on the plot? It would be easier to follow if the text and the figure matched up.*

We agree with the reviewer on this comment. The text has been amended to match the colour bar for ease of comparison.

Page 8733 Line 1-2: explain “mean fractional difference”

What we mean by ‘mean fractional difference’ is the mean (or median in line 2) of the relative difference of age to the size of the effective physical age (age differences/physical ages) for both within and outwith the plume. We agree with the reviewer that this needs more explanation . We have been split the statement into two separate points to make our message clearer as well as updating the numbers to correspond with the new higher resolution nested results.

Page 8733 Line 18-19: First mention of sub-grid scale vertical mixing. Why do you come to this conclusion. Maybe better to explain earlier in the manuscript or and least explain it here.
The model bias can be partially explained by the sub-grid scale vertical mixing. The model injection height of the smoke plume, in the absence of other information, remains in the boundary layer while in reality the majority of pollutants could be injected into the free troposphere. This has implications for the subsequent atmospheric transport of emitted gases. We have now improved this explanation in the revised manuscript.

Page 8734 Line 12 - 15: have you described this HYSPLIT evidence earlier in the text? Explain this more clearly - We have not explained it earlier in the text. Here we simply use this as a comparison with a paper (Griffin et al, 2013) where HYSPLIT is used briefly to estimate the age of pollutants they observed. We have now explained this further in the manuscript in the concluding remarks.

Manuscript prepared for Atmos. Chem. Phys.
with version 4.2 of the LaTeX class copernicus.cls.
Date: 8 October 2014

Origin, variability and age of biomass burning plumes intercepted during BORTAS-B

D. P. Finch[1], P. I. Palmer[1], and M. Parrington[1,2]

[1]School of GeoSciences, University of Edinburgh, UK
[2]Now at the European Centre for Medium-range Weather Forecasts, Reading, UK

Correspondence to: D. P. Finch
(d.finch@ed.ac.uk)

Abstract.

We use the GEOS-Chem atmospheric chemistry transport model to interpret aircraft measurements of carbon monoxide (CO) in biomass burning outflow taken during the 2011 BORTAS-B campaign over eastern Canada. The model has some skill reproducing the observed variability (Spearmans rank correlation r_s = 0.65 but has a positive (negative) bias for observations <100 ppb (>300 ppb). We find that observed CO variations are largely due to NW North American biomass burning, as expected, with smaller and less variable contributions from fossil fuel combustion from eastern Asia and NE North America. To help interpret observed variations of CO we develop an Eulerian effective physical age of emissions ($\bar{A}$) metric, accounting for mixing and chemical decay, which we apply to pyrogenic emissions of CO. We find that during BORTAS-B the age of emissions intercepted over Halifax, Nova Scotia is typically 4–11 days, and on occasion as young as two days. We show that $\bar{A}$ is typically 1–5 days older than the associated photochemical ages inferred from colocated measurements of different hydrocarbons. We find that the median difference between the age measures ($\Delta\tau$) in plumes (CH_3CN>150 ppt) peaks at 3 days. This corresponds to a chemical retardation of 50%. We find a strong relationship in biomass burning plumes between $\bar{A}$ and $\Delta\tau$ (r^2=0.80), which is not present outwith these plumes (r^2=0.28). We argue that these observed relationships, together with a robust observed relationship between CO and black carbon aerosol during BORTAS-B (r^2 >0.7), form the basis of indirect evidence that aerosols co-emitted with gases during pyrolysis markedly slowed down the plume photochemistry during BORTAS-B with respect to photochemistry at the same latitude and altitude in clear skies.

1 Introduction

The open burning of biomass is an inefficient combustion process, resulting in the release of a wide range of chemically reactive gases and particles that contribute to the production of ozone in the troposphere (Goode et al., 2000; Koppmann et al., 2005; Akagi et al., 2011), with implications for national surface air quality and air quality mitigation strategies. However, the rate and extent of photochemical ozone production in biomass burning outflow is still a matter of debate that largely reflects the sensitivity of results to environmental conditions (Jaffe and Wigder, 2012). In this paper we present an analysis of measurements of carbon monoxide (CO) from the BORTAS-B aircraft campaign during July 2011 (Palmer et al., 2013), in conjunction with a 3-D chemistry transport model to understand the processes that determine observed CO variability and relate the ages of emissions to the observed photochemical production of ozone.

Ozone production within biomass burning plumes intercepted during the BORTAS-B campaign (Palmer et al., 2013) has previously been studied using photochemical age (Parrington et al., 2013; Parrish et al., 2007). Estimating the photochemical age of a pyrogenic airmass relies on an accurate knowledge of the OH radical, and assumes constant trace gas emission factors from pyrogenic processes. However, despite these weaknesses the photochemical age is still a useful metric for helping to interpret observed trace gas variations. We introduce a complementary (weighted-mean) effective physical age metric $\bar{A}$. Using $\bar{A}$ we can infer age distributions within an airmass and by comparing $\bar{A}$ with the photochemical age we can estimate how the physical and chemical environment of the plume has modified the speed of the in situ plume chemistry.

The main source of CO is from the incomplete combustion of fossil fuel, biomass, and biofuel. There is also a source of CO from the oxidation from methane and non-methane volatile organic compounds (NMVOCs) (Duncan et al., 2007). The main sink is from the oxidation by the hydroxyl radical (OH), resulting in an atmospheric lifetime of weeks to months depending on latitude and season. We use airborne CO measurements from phase B of the Quantifying the impacts of BOReal forest fires on Tropospheric oxidants over the Atlantic using Aircraft and Satellites (BORTAS-B) project, July 2011. The overall objective of BORTAS was to better understand the production of tropospheric ozone in respect to the chemical evolution of plumes from boreal forest fires, which was achieved by integrating aircraft (Lewis et al., 2013; Le Breton et al., 2013; O'Shea et al., 2013), surface (Gibson et al., 2013; Griffin et al., 2013), sonde (Parrington et al., 2012), and satellite measurements Tereszchuk et al. (2013) of atmospheric composition. Phase A of BORTAS was conducted without aircraft in July 2010 (Parrington et al., 2012).

In the next section we briefly describe the CO data we analyse. The GEOS-Chem chemistry transport model is described in section 3, including a description of a new age of emission calculation which we use to interpret the data. Our results are reported in section 4, including a statistical analysis of the data and a model interpretation of the data. We conclude in section 5.

2 Data and Methods

2.1 BORTAS-B Carbon Monoxide and CH_3CN Data

Here we use data exclusively from the BORTAS-B aircraft campaign. The focus of the work shown here is the analysis of CO measurements, which are operated by the Facility for Airborne Atmospheric Measurements on the BAe-146 atmospheric research aircraft using a fast-response vacuum-UV resonance fluorescence instrument (Gerbig et al., 1999). The instrument has an averaging time of 1 s and a precision and accuracy of 1 ppb and 3%, respectively. We use measurements of acetonitrile (CH_3CN, not shown), an additional tracer of biomass burning, measured by Proton Transfer Reaction Mass Spectrometer (Murphy et al., 2010) to isolate plumes within BORTAS-B. These measurements have a mean precision of 37 ppt during BORTAS-B (Palmer et al., 2013). We define plumes as CO measurements corresponding to CH_3CN>150 ppt.

2.2 The GEOS-Chem Atmospheric Chemistry Model

We use the GEOS-Chem atmospheric chemistry model (www.geos-chem.org) to interpret the BORTAS-B CO measurement. The model has been documented extensively (e.g., Bey et al. (2001); Duncan et al. (2007); Gonzi et al. (2011); Parrington et al. (2012)) and here we only include those details relevant to our study.

We use v9-01-03 of the model, driven by GEOS-5 assimilated meteorological data from the NASA Global Modelling and Assimilation Office (GMAO) Goddard Earth Observing System (GEOS). For global simulations we use a spatial resolution of 2° latitude by 2.5° longitude (a degradation of the native resolution of 0.5°×0.667°) with 47 vertical levels with a temporal resolution of 30 minutes. For the model runs we use to compare against BORTAS-B aircraft data and the $\bar{A}$ calculations we use the the native model resolution with 47 vertical levels. We use the Global Fire Emissions Database (GFED-3), describing biomass burning emissions (Giglio et al., 2010), which has a three-hour temporal resolution; fossil fuel emissions from the Emissions Database for Global Atmospheric Research (EDGAR, Olivier et al. (1999)); and biogenic emissions from the Model of Emissions of Gases and Aerosol from Nature (MEGAN, Guenther et al. (2006)). We report model calculations from the summers (JJA) of 2008–2011. We initialize the model in 2007, using previous model output, and run using a single total CO tracer for 9 months until our study period JJA 2008. During the summer periods we use "tagged" tracers (described below) and between the successive summer periods we collapse these tagged tracers back to the single tracer for computational expediency.

For the CO attribution calculations, we use a "tagged" version of the model (e.g., Jones et al. (2003); Palmer et al. (2003, 2006); Feng et al. (2009); Fisher et al. (2010)), which uses pre-calculated monthly 3-D OH fields. Using these fields allows us to linearly decompose the CO originating from specific processes and geographical regions. Figure 1 shows the geographical regions we use. For biomass burning in the northern hemisphere we split North America into four quadrants, consider

Europe as one region, and split Russia/Siberia into three regions (western, mid, and eastern). We show below that most of the observed CO over eastern Canada during JJA originates from these regions. For northern hemisphere fossil fuel we have combined some regions that do not play a significant role the interpretation of the BORTAS-B data. The chemical source of CO from the oxidation of methane and NMVOCs is treated as one global tracer. In total, we have 28 tracers (including the background) that sum to the total atmospheric CO. Wherever we compare the model against data we sample the model at the time and location of the measurement.

2.3 Age of Emission Model Calculation

We use the same model structure for the "tagged" CO simulation to calculate $\bar{A}$. To calculate $\bar{A}$, we adapt the model to instead emit an arbitrary constant amount to a day-specific tracer wherever there is active burning during our study period (informed by GFED-3). Once emitted the tracer is left to disperse. We assume a constant chemical lifetime of 60 days from the oxidation by OH, corresponding to an OH concentration of 1.9×10^{6} molec/cm^{-3}. At the end of a 31-day simulation for July, say, we have 31 tracers. The age of each tracer is simply the number of days since the start of the run minus the tracer number (not value).

To account for older air being subject to more dispersion than younger air we define an effective age of air $\bar{A}$:

$$\bar{A} = \frac{\sum_i A_i L_{M,i} L_{C,i}}{\sum_i L_{M,i} L_{C,i}}, \tag{1}$$

which represents a weighted mean of the age of each tracer A_i, the value of each tracer $L_{M,i}$ that is a measure of atmospheric mixing processes, and the chemical lifetime of each tracer $L_{C,i}$. More generally, we can extend this formulation to include other sink terms such as, for example, dry and wet deposition. For $L_{C,i}$ we assume a constant chemical lifetime of 60 days as described above. This method does not account for the magnitude of CO emitted from any fire, regardless of its size.

For this paper, calculating $\bar{A}$ allows us to quantify the physical age of emissions intercepted during BORTAS-B, providing additional information to interpret the chemical signature of the sampled air masses. It also allows us to determine whether the air masses intercepted during BORTAS-B were representative of that summer and of a similar period from preceding years.

We compare our $\bar{A}$ estimates against the associated photochemical ages of plumes intercepted in BORTAS-B (Parrington et al., 2013). The photochemical age is the time taken for a tracer to be photochemically removed from a biomass burning plume. It is based on ratios of NMVOCs close to the emission source (here, determined by flight B626 in the BORTAS-B campaign over Northwestern Ontario on the 26th July 2011) and the ratio of NMVOCs at the time of observations. Assuming a representative OH value, an age determined solely by photochemistry can be calculated for a plume.

3 Results

3.1 Statistical Analysis of BORTAS-B CO Data

Figure 2 show the mean statistics of the nested model and observed CO concentrations during BORTAS-B. Mean and median values of observed CO suggests the model has a small positive bias; mean (median) model minus observed CO residual of 18.4 ppb (-0.1 ppb). We find the model has a positive bias below observations of 100 ppb and a negative bias for observations >300 ppb. The largest discrepancies between the model and the observations generally occur at the largest values of CO. The 99th percentile value for model and observed CO concentrations are 670 ppb and 436 ppb, respectively. The interquartile range for BORTAS-B observed CO is 87–133 ppb with a mode of 87 ppb. This is consistent with background CO measurements during the NASA ARCTAS-B campaign (Arctic Research of the Composition of the Troposphere from Aircraft and Satellites, Jacob et al. (2010)). The largest observed CO concentrations during BORTAS-B are larger than those observed during ARCTAS-B (Liang et al., 2011). Figure 3 shows that the relative model error [model minus observation]/model is typically within ± 0.5 but has a range of ± 1.0. The model overestimates observed CO concentrations between the surface and 800 hPa, reflecting the outflow of anthropogenic and biomass burning pollution, with the largest discrepancy around 800 hPa. The model generally has more skill in reproducing the variability of observed CO during BORTAS-B in the below 4 km (Spearman's rank correlation r_s = 0.65) than above 4 km (r_s = 0.19). We use Spearman's rank correlation because it is a more appropriate metric that can describe the model ability to reproduce qualitatively observed elevated values (plumes) above a background but not necessarily capture the value of these elevated values. The inability of the model to capture these elevated values may reflect errors in emissions or atmospheric transport.

3.2 Tagged CO Model Output

Table 1 shows the tagged model analysis sampled at the times and locations of the BORTAS-B CO measurements. The largest source of CO and the largest source of CO variability during BORTAS was from NE North American biomass burning, as expected. There are also large but much less variable contributions from the background (air older than JJA) and from the oxidation of methane and NMVOCs. CO produced by CH_4 oxidation typically contributes around 30% to global concentrations (Duncan et al., 2007).

Figure 4 shows the mean JJA model contributions of total surface CO from different geographically based sources 2008–2011, described using a horizontal resolution of 2° latitude by 2.5° longitude. The contribution from biomass burning over NW North America is broadly constant from year to year, although the distribution of the fires varies substantially, with Alaska playing a dominant role only in 2009 during our study period. The magnitude and the distribution of fossil fuel emissions from NE North America (predominately the NE USA) appear reasonably consistent over

the four years, with emissions generally travelling up the eastern seaboard with eventual outflow to the Atlantic ocean close to Halifax, Nova Scotia. Similar to North America, Siberian biomass burning has substantial spatial variability from year to year, with their location playing a key role in determining their eventual impact on North America and Europe. During 2010 the largest CO concentrations originated from East Siberia and spread across the northern hemisphere. In contrast, during BORTAS-B in 2011 most of the fire activity was further SW and had less of an impact over eastern Canada. Fires from mid-Siberia had a larger influence on total CO during 2008–2009, with very little activity during 2010–2011. There is a consistently small source from fossil fuel combustion from East Asia (not shown), peaking at around 400 ppb over China but quickly dropping off to around 10 ppb by the time it has crossed the Pacific. Differences between Figure 4 and Figure 9 from Palmer et al. (2013), also showing polar CO concentrations during BORTAS-B, are due to different biomass burning inventories. Here, we use GFED-3 (see above) and Palmer et al. (2013) used the Fire Locating and Modeling of Burning Emissions inventory (Reid et al., 2009).

Figure 5 shows that biomass burning from the NW North America is still a dominant factor in the variability of total CO in the free troposphere. During 2010, these fires contributed around 50 ppb of CO into the upper troposphere causing widespread pollution during July. Typically these emissions contribute about 10 ppb of CO over Europe. Contributions from east and mid Siberia appear to be consistent over the four years except during 2010 when there is very little material transported into the free troposphere. In general, the magnitude and distribution of the fossil fuel source is consistent across the four years with weather systems lifting up surface emission to the free troposphere.

The widespread and persistent source of CO (approximately 10 ppb) from Asian anthropogenic sources over the northern hemisphere (not shown) agrees with the ARCTAS-A study (Fisher et al., 2010) and ARCTAS-B (Bian et al., 2013). Relative to ARCTAS-A, BORTAS-B generally shows a much larger contribution to the total CO from boreal biomass burning, reflecting the timing of ARCTAS-A in April 2008 before the beginning of the main fire season. For JJA 2008–2011 we find boreal biomass burning represents a significant contribution to the total surface CO over the Western Arctic region defined as 50°N–90°N, 170°W–40°W, following Bian et al. (2013). Analysis of ARCTAS-B data showed that boreal biomass burning contributed approximately 25% of CO in this region during July 2008 (Bian et al., 2013). We find boreal biomass burning contributes 25%–45% of the total CO for the defined Western Arctic region for all years, peaking at >90% of the total CO over intense burning areas. During 2008 we find our results are broadly consistent with Bian et al. (2013) but at the lower end of their range. The discrepancy between these results is likely due to using different emission inventories, with Bian et al. (2013) using the Quick Fire Emissions Database.

3.3 Effective Physical Age of Air

Figure 6 shows the mean model statistics for $\bar{A}$ during July 2008–2011 at 95°W and 50°W, averaged over 45°–60°N, representing the approximate western and eastern boundaries of the measurements sampled during BORTAS-B. We consider four altitude bins, corresponding to the boundary layer (0–2 km), lower and mid troposphere (2–4 km and 4–6 km, respectively), and upper troposphere (>6 km). At the western boundary, emissions from 2008 have a median age of seven days, 2009 has a median age of 10 days, and 2010 and 2011 have a median age of five days. We find the older age of emissions during 2009 is due to fewer fires along the western boundary and consequently a larger influence from Alaska and further afield. Air sampled at the eastern boundary is older, as expected with the except of the upper troposphere (>6 km) which shows similar medians from the western boundary to the eastern boundary. The eastern boundary for all years and at all altitudes have median values between 11 and 13 days and a range of 2–23 days. The difference in $\bar{A}$ between the two boundaries decreases with altitude; above 4 km, ages are indistinguishable because air is more well-mixed and influenced by emissions outside of the domain. The age of emissions clearly get older moving towards the Atlantic, with an increase in median age of approximately three days for all years except 2009, when the age difference between the west and east boundaries is approximately one day in the lower troposphere and insignificant at higher altitudes. We attribute this lack of ageing in 2009 to fewer Canadian fires during July of this year, as mentioned above. Boreal biomass burning in 2009 started earlier in the year and was more prominent in Alaska and Siberia. Emissions tend to be older at 50°W at lower altitudes (not shown). This may be a result from fresher emissions getting lofted higher into the atmosphere as they travel. Figure 6 also shows that the median value of $\bar{A}$ (six days) sampled during BORTAS-B falls within the range of model emission ages at 95°W, with the majority of measurements taken 65°–40°W. We find a similar observed median value of $\bar{A}$ for all altitudes, which is typically lower than the model free troposphere. This bias towards younger ages reflects the sampling strategy of BORTAS-B that was to intercept fresh biomass biomass plumes.

Figure 7 shows an example of $\bar{A}$ on 20th July 2011, which is used as a case study in other BORTAS studies (e.g., Griffin et al. (2013); Franklin et al. (2014)). The longitudinal cross section shows fresh emissions from the Thunder Bay region (50°N, 88°W), peaking at approximately a week old on the 20th of July (corresponding to the 14th–15th July), that eventually age as they are transported eastwards. When they were intercepted by the surface measurements over Toronto (43.70°N, 69.40°W) (Griffin et al., 2013) and Halifax (44.6°N, 63.59°W) (Franklin et al., 2014) emissions are typically 5–7 days old. Figure 7 shows the transported air, intercepted at 63°W, is composed of a young plume (4–5 days old) surrounded by older air (seven days old) over 47°–55°N. Previous analysis used the NOAA HYbrid Single-Particle Lagrangian Integrated Trajectory (HYSPLIT) model (Draxler and Hess, 1998), driven by meteorological reanalyses data from the National Center for Environmental Prediction (NCEP) Global Data Assimilation Program (GDAS), to interpret ground-based remote-sensing data collected during BORTAS-B (Griffin et al., 2013; Franklin et al., 2014).

We find our Eulerian age of emission estimates are typically a day older than those determined by the the HYSPLIT model during the 19–21 July 2011 when ground-based observations reported elevated concentrations due to biomass burning (Gibson et al., 2013; Griffin et al., 2013; Franklin et al., 2014).

Figure 8 shows the mean statistics of $\bar{A}$ intercepted during BORTAS-B are generally consistent with the associated median photochemical age, determined using NMVOC ratios, of six days (Parrington et al., 2013). The photochemical ages range 0–16 days while $\bar{A}$ has a range of 2–14 days. There are substantial differences between the photochemical and $\bar{A}$ for each flight. Figure 9 shows that $\bar{A}$ minus photochemical age ($\Delta\tau$) have distinct frequency distributions within and outwith plumes. Within plumes, the distribution peaks at $\Delta\tau$=2–4 days (median 1.8 days), while outwith plumes there is a relatively flat distribution. We find no significant difference to our results if we average the photochemical ages onto the model grid prior to the analysis. Figure 9 shows that high values of CO relate to $\Delta\tau$ of 2–4 days, corresponding to a mean (median) fractional difference of 0.44 (0.40); and a weaker relationship between $\Delta\tau$ outwith plumes, corresponding to a mean (median) fractional difference of 0.11 (0.10). Figure 9 also shows that $\Delta\tau$ increases with $\bar{A}$ within plumes (r^2=0.80) from close to zero at 3–4 days to >5 days for plumes older than 10 days. There is a much weaker relationship between these two age variables outwith plumes (r^2=0.28).

4 Concluding Remarks

We used the GEOS-Chem global atmospheric chemistry model to interpret observed variations of CO taken during the BORTAS-B aircraft campaign over eastern Canada in July-August 2011. We reported a mean difference between the observations and the model for the whole atmosphere of 18.4 ppb and a median of -0.1 ppb. The distribution of these residuals has a high kurtosis, with the majority of residuals within 50 ppb of the mean value. The model has a positive bias below observed values of 100 ppb and a negative bias above 300 ppb. We found that the larger differences between the model and the observations in the mid troposphere, where we found pyrogenic CO peaked. The model has some skill at reproducing the mean observed statistics in the lower troposphere (Spearman's rank correlation r_s = 0.65), and less skill in the higher troposphere (r_s = 0.19). The difference in model skill at different altitudes is likely due to a) misdiagnosing sub-gridscale vertical mixing of pyrogenic material lofted by surface heating due to fires, and b) errors in biomass burning emission inventories.

Using a linearly-decomposed version of the model we found that most of the observed variability in CO concentration during BORTAS-B was due to Canadian biomass burning, as expected, with a smaller contribution from Siberian biomass burning and NE North American fossil fuel combustion. We used the model to put BORTAS-B into the wider temporal context of 2008–2011. We found that North American biomass burning is broadly constant (45% of total CO) over this period although the

spatial distribution of fires varies substantially. The variation of Siberian biomass burning is more extreme with large contributions to total CO over North American during some years (2008–2009) and very little activity in other years (2010–2011), reflecting the spatial extent and geographical position of the fires. Based on our analysis of the source contributions to North American CO over during the (limited) four-year period we conclude that BORTAS-B (2011) was not anomalous.

Previous work has shown that ozone production within biomass burning plumes can be described using photochemical ageing (Parrington et al., 2013). In this paper we describe a new Eulerian method to quantify the effective physical age of emissions $\bar{A}$, taking into account mixing and chemical decay of emitted air masses of varying age. We found that during BORTAS-B, values of $\bar{A}$ for airmasses intercepted over Halifax, Nova Scotia are typically 4–11 days old but occasionally as young as two days, corresponding well to analysis of concurrent ground-based observations at the Dalhousie ground station (DGS) in Halifax, NS (Gibson et al., 2013). We found our Eulerian age of emission estimates are typically a day older than those determined by the the HYSPLIT model during the 19–21 July 2011 when ground-based observations reported elevated concentrations due to biomass burning (Gibson et al., 2013; Griffin et al., 2013; Franklin et al., 2014). We attributed this difference in age to our method accounting for older air masses that are not explicitly considered by HYSPLIT. We compared the values of $\bar{A}$ calculated using our method to the corresponding photochemical ages, using ratios of NMVOCs (Parrington et al., 2013), and found that values of $\bar{A}$ are typically 1–5 days older. We found that the median difference between the age measures in plumes (defined as CH_3CN>150 ppt) peaks at 3–5 days, compared to a muted distribution for background CO concentrations, corresponding to a chemical retardation of 50%. We also found that in plumes $\Delta\tau$ increased with physical age (r^2=0.80), which was much less pronounced outwith plumes (r^2=0.23). Based on $\Delta\tau$ within and outwith plumes and on a strong relationship between CO and, for example, black carbon aerosol during BORTAS-B (r^2 >0.70, Taylor et al. (2014)) we hypothesize that $\Delta\tau$ variations provide evidence that pyrogenic aerosols slow down the plume photochemistry for many days downwind from the point of burning.

Previous work has showed using a photochemical model that the observed ozone tendency of Alaskan forest fire plumes observed over the North Atlantic during 2004 was consistent with a reduced photolysis rate of approximately 20% that could be due to aerosol loading within/above these plumes (Real et al., 2007). Our analysis of photochemical age versus $\bar{A}$ suggests a larger retardation to the plume photochemistry. One important counter argument to our analysis of $\Delta\tau$ that could reconcile $\bar{A}$ and photochemical ages is that the photochemical age could have a negative bias. The method, described in detail by Parrington et al. (2013), relies on variation of NMVOC ratios that have different chemical lifetimes against oxidation by OH. The lifetime calculation is anchored by an assumption of a constant OH concentration. The BORTAS-B data analysis assumed an OH concentration of 2×10^6 molec/cm^3 that was chosen to be representative of a northern midlatitude summertime OH concentration (Spivakovsky et al., 2000). Halving (doubling) the assumed OH con-

centration would increase (decrease) the photochemical age. For many flights the median value of $\bar{A}$ is substantial higher than the photochemical age. As discussed in Yokelson et al. (2013), there are inherit limitations to using photochemistry as a proxy for the age of emissions. The photochemical age calculation also assumes a constant emission ratio of NMVOCs from the fires, and a constant background concentration. Our method also assumes constant OH concentrations, but it is much less sensitive to changes in OH concentration. All values of $\bar{A}$ we report in our domain are well within the e-folding lifetime set by OH therefore diffusion is the dominant effect on $\bar{A}$ for our time scale. By running our analysis with a doubled and halved lifetime of CO against OH oxidation we find that values of $\bar{A}$ differ by less than one day.

Our method of calculating $\bar{A}$ does not consider the size of the fire or the amount of CO that is emitted. While this will not affect the $\bar{A}$ calculation it may complicate the interpretation of data. If, for example, old, high-CO air masses mix with young, low-CO air masses our method will assign more weight to the younger air mass and a stronger attribution to the observed CO variability. We tried to minimize this issue by using a fixed chemical decay but some residual of this issue will unavoidably remain. Other measures of age inferred from Lagrangian back trajectories, say, will suffer from similar problems and in some circumstances be more problematic if the mixing of different air masses is not considered.

Accounting for biomass burning in regional air quality budgets downwind of fires presents a number of challenges, not least due to the ability of models to predict where plume chemistry will result in net production of O_3. It is well established that this production is a function of the pyrogenic emissions (themselves a function of many environmental variables), the associated vertical mixing and transport pathways, and the photochemical environment. Using BORTAS-B we have only inferred that aerosols have slowed photochemical ageing of plumes but there is insufficient data to characterize directly how the aerosols have affected the photochemical environment within the plume as a function of time. Further studies of similar pyrogenic plumes should include a full suite of aerosol and radiation instruments in addition to gas-phase atmospheric chemistry instruments. This kind of integrative analysis will become progressively more important as we analyze more complex environments such as megacities where there is typically a mix of biogenic, anthropogenic, and pyrogenic material determining ozone photochemistry.

Acknowledgements. This research was supported by the Natural Environment Research Council under grant number NE/F017391/1. DF acknowledges NERC studentship NE/K500835/1. PIP acknowledges support from his Philip Leverhulme Prize and his Royal Society Wolfson Research Merit Award. DF and PIP designed the numerical calculations, performed the analysis, and wrote the paper; PIP was also the principal BORTAS mission scientist. MP was a mission scientist on BORTAS, and provided the photochemical ages and comments on the paper.

References

Akagi, S. K., Yokelson, R. J., Wiedinmyer, C., Alvarado, M. J., Reid, J. S., Karl, T., Crounse, J. D., and Wennberg, P. O.: Emission factors for open and domestic biomass burning for use in atmospheric models, Atmos. Chem. Phys., 11, 4039–4072, doi:10.5194/acp-11-4039-2011, http://www.atmos-chem-phys.net/11/4039/2011/, 2011.

Bey, I., Jacob, D. J., Yantosca, R. M., Logan, J. a., Field, B. D., Fiore, A. M., Li, Q., Liu, H. Y., Mickley, L. J., and Schultz, M. G.: Global modeling of tropospheric chemistry with assimilated meteorology: Model description and evaluation, J. Geophys. Res., 106, 23 073, doi:10.1029/2001JD000807, http://doi.wiley.com/10.1029/2001JD000807, 2001.

Bian, H., Colarco, P. R., Chin, M., Chen, G., Rodriguez, J. M., Liang, Q., Blake, D., Chu, D. a., da Silva, A., Darmenov, a. S., Diskin, G., Fuelberg, H. E., Huey, G., Kondo, Y., Nielsen, J. E., Pan, X., and Wisthaler, A.: Source attributions of pollution to the Western Arctic during the NASA ARCTAS field campaign, Atmos. Chem. Phys., 13, 4707–4721, doi:10.5194/acp-13-4707-2013, http://www.atmos-chem-phys.net/13/4707/2013/, 2013.

Draxler, R. R. and Hess, G. D.: An overview of the HYSPLIT 4 modeling system of trajectories, dispersion, and deposition, Aust. Meteor. Mag., 47, 295–308, 1998.

Duncan, B. N., Logan, J. a., Bey, I., Megretskaia, I. a., Yantosca, R. M., Novelli, P. C., Jones, N. B., and Rinsland, C. P.: Global budget of CO, 1988âĂŞ1997: Source estimates and validation with a global model, J. Geophys. Res., 112, D22 301, doi:10.1029/2007JD008459, http://doi.wiley.com/10.1029/2007JD008459, 2007.

Feng, L., Palmer, P. I., Bösch, H., and Dance, S.: Estimating surface CO2 fluxes from space-borne CO2 dry air mole fraction observations using an ensemble Kalman Filter, Atmos. Chem. Phys., 9, 2619–2633, doi:10.5194/acp-9-2619-2009, http://www.atmos-chem-phys.net/9/2619/2009/, 2009.

Fisher, J. a., Jacob, D. J., Purdy, M. T., Kopacz, M., Le Sager, P., Carouge, C., Holmes, C. D., Yantosca, R. M., Batchelor, R. L., Strong, K., Diskin, G. S., Fuelberg, H. E., Holloway, J. S., Hyer, E. J., McMillan, W. W., Warner, J., Streets, D. G., Zhang, Q., Wang, Y., and Wu, S.: Source attribution and interannual variability of Arctic pollution in spring constrained by aircraft (ARCTAS, ARCPAC) and satellite (AIRS) observations of carbon monoxide, Atmos. Chem. Phys., 10, 977–996, doi:10.5194/acp-10-977-2010, http://www.atmos-chem-phys.net/10/977/2010/, 2010.

Franklin, J. E., Drummond, J. R., Griffin, D., Pierce, J. R., Waugh, D. L., Palmer, P. I., Parrington, M., Lee, J. D., Lewis, A. C., Rickard, A. R., Taylor, J. W., Allan, J. D., Coe, H., Walker, K. A., Chisholm, L., Duck, T. J., Hopper, J. T., Blanchard, Y., Gibson, M. D., Curry, K. R., Sakamoto, K. M., Lesins, G., Dan, L., Kliever, J., and Saha, A.: A case study of aerosol depletion in a biomass burning plume over Eastern Canada during the 2011 BORTAS field experiment, Atmospheric Chemistry and Physics Discussions, 14, 3395–3426, doi:10.5194/acpd-14-3395-2014, http://www.atmos-chem-phys-discuss.net/14/3395/2014/, 2014.

Gerbig, C., Schmitgen, S., Kley, D., Volz-Thoms, A., Dewey, K., Haaks, D., and Volz-Thomas, A.: An improved fast-response vacuum-UV resonance fluorescence CO instrument, J. Geophys. Res., 104, 1699–1704, doi:10.1029/1998JD100031, http://doi.wiley.com/10.1029/1998JD100031, 1999.

Gibson, M. D., Pierce, J. R., Waugh, D., Kuchta, J. S., Chisholm, L., Duck, T. J., Hopper, J. T., Beauchamp, S., King, G. H., Franklin, J. E., Leaitch, W. R., Wheeler, A. J., Li, Z., Gagnon, G. A., and Palmer, P. I.:

Identifying the sources driving observed PM_{2.5} temporal variability over Halifax, Nova Scotia, during BORTAS-B, Atmos. Chem. Phys., 13, 7199–7213, 2013.

Giglio, L., Randerson, J. T., van der Werf, G. R., Kasibhatla, P. S., Collatz, G. J., Morton, D. C., and DeFries, R. S.: Assessing variability and long-term trends in burned area by merging multiple satellite fire products, Biogeosciences, 7, 1171–1186, doi:10.5194/bg-7-1171-2010, http://www.biogeosciences.net/7/1171/2010/, 2010.

Gonzi, S., Feng, L., and Palmer, P. I.: Seasonal cycle of emissions of {CO} inferred from {MOPITT} profiles of {CO}: Sensitivity to pyroconvection and profile retrieval assumptions, Geophys. Res. Lett., 38, 2011.

Goode, J. G., Yokelson, R. J., Ward, D. E., Susott, R. A., Babbitt, R. E., Davies, M. A., and Hao, W. M.: Measurements of excess O3 , CO2 , CO, CH4 , C2H4 , C2H2 , HCN, NO, NH 3 , HCOOH, CH3 COOH, HCHO, and CH 3 OH in 1997 Alaskan biomass burning plumes by airborne Fourier transform infrared spectroscopy (AFTIR), J. Geophys. Res., 105, 22 147, doi:10.1029/2000JD900287, http://doi.wiley.com/10.1029/2000JD900287, 2000.

Griffin, D., Walker, K. a., Franklin, J. E., Parrington, M., Whaley, C., Hopper, J., Drummond, J. R., Palmer, P. I., Strong, K., Duck, T. J., Abboud, I., Bernath, P. F., Clerbaux, C., Coheur, P.-F., Curry, K. R., Dan, L., Hyer, E., Kliever, J., Lesins, G., Maurice, M., Saha, a., Tereszchuk, K., and Weaver, D.: Investigation of CO, C₂H₆ and aerosols in a boreal fire plume over eastern Canada during BORTAS 2011 using ground- and satellite-based observations and model simulations, Atmos. Chem. Phys., 13, 10 227–10 241, doi:10.5194/acp-13-10227-2013, http://www.atmos-chem-phys.net/13/10227/2013/, 2013.

Guenther, A., Karl, T., Harley, P., Wiedinmyer, C., Palmer, P. I., and Geron, C.: Estimates of global terrestrial isoprene emissions using MEGAN (Model of Emissions of Gases and Aerosols from Nature), Atmos. Chem. Phys. Discuss., 6, 107–173, doi:10.5194/acpd-6-107-2006, http://www.atmos-chem-phys-discuss.net/6/107/2006/, 2006.

Jacob, D. J., Crawford, J. H., Maring, H., Clarke, a. D., Dibb, J. E., Emmons, L. K., Ferrare, R. a., Hostetler, C. a., Russell, P. B., Singh, H. B., Thompson, a. M., Shaw, G. E., McCauley, E., Pederson, J. R., and Fisher, J. a.: The Arctic Research of the Composition of the Troposphere from Aircraft and Satellites (ARCTAS) mission: design, execution, and first results, Atmos. Chem. Phys., 10, 5191–5212, doi:10.5194/acp-10-5191-2010, http://www.atmos-chem-phys.net/10/5191/2010/, 2010.

Jaffe, D. a. and Wigder, N. L.: Ozone production from wildfires: A critical review, Atmos. Environ., 51, 1–10, doi:10.1016/j.atmosenv.2011.11.063, http://linkinghub.elsevier.com/retrieve/pii/S1352231011012507, 2012.

Jones, D. B. a., Bowman, K. W., Palmer, P. I., Worden, J. R., Jacob, D. J., Hoffman, R. N., Bey, I., and Yantosca, R. M.: Potential of observations from the Tropospheric Emission Spectrometer to constrain continental sources of carbon monoxide, J. Geophys. Res. Atmos., 108, n/a—-n/a, doi:10.1029/2003JD003702, http://doi.wiley.com/10.1029/2003JD003702, 2003.

Koppmann, R., von Czapiewski, K., and Reid, J. S.: A review of biomass burning emissions, part I: gaseous emissions of carbon monoxide, methane, volatile organic compounds, and nitrogen containing compounds, Atmos. Chem. Phys. Discuss., 5, 10 455–10 516, doi:10.5194/acpd-5-10455-2005, http://www.atmos-chem-phys-discuss.net/5/10455/2005/, 2005.

Le Breton, M., Bacak, A., Muller, J. B. A., O'Shea, S. J., Xiao, P., Ashfold, M. N. R., Cooke, M. C., Batt, R., Shallcross, D. E., Oram, D. E., Forster, G., Bauguitte, S. J.-B., Palmer, P. I., Parrington, M., Lewis,

A. C., Lee, J. D., and Percival, C. J.: Airborne hydrogen cyanide measurements using a chemical ionisation mass spectrometer for the plume identification of biomass burning forest fires, Atmos. Chem. Phys., 13, 9217–9232, 2013.

Lewis, A. C., Evans, M. J., Hopkins, J. R., Punjabi, S., Read, K. A., Purvis, R. M., Andrews, S. J., Moller, S. J., Carpenter, L. J., Lee, J. D., Rickard, A. R., Palmer, P. I., and Parrington, M.: The influence of biomass burning on the global distribution of selected non-methane organic compounds, Atmos. Chem. Phys., 13, 851–867, 2013.

Liang, Q., Rodriguez, J. M., Douglass, A. R., Crawford, J. H., Olson, J. R., Apel, E., Bian, H., Blake, D. R., Brune, W., Chin, M., Colarco, P. R., da Silva, A., Diskin, G. S., Duncan, B. N., Huey, L. G., Knapp, D. J., Montzka, D. D., Nielsen, J. E., Pawson, S., Riemer, D. D., Weinheimer, A. J., and Wisthaler, A.: Reactive nitrogen, ozone and ozone production in the Arctic troposphere and the impact of stratosphere-troposphere exchange, Atmospheric Chemistry and Physics, 11, 13 181–13 199, doi:10.5194/acp-11-13181-2011, 2011.

Murphy, J. G., Oram, D. E., and Reeves, C. E.: Measurements of volatile organic compounds over West Africa, Atmospheric Chemistry and Physics, 10, 5281–5294, doi:10.5194/acp-10-5281-2010, http://www.atmos-chem-phys.net/10/5281/2010/, 2010.

Olivier, J. G. J., Bloos, J. P. J., Berdowski, J. J. M., Visschedijk, A. J. H., and Bouwman, A. F.: A 1990 global emission inventory of anthropogenic sources of carbon monoxide on 1ÂřÃŮ1Âř developed in the framework of EDGAR/GEIA, Chemosph. - Glob. Chang. Sci., 1, 1–17, doi:10.1016/S1465-9972(99)00019-7, http://linkinghub.elsevier.com/retrieve/pii/S1465997299000197, 1999.

O'Shea, S. J., Allen, G., Gallagher, M. W., Bauguitte, S. J.-B., Illingworth, S. M., Le Breton, M., Muller, J. B. A., Percival, C. J., Archibald, A. T., Oram, D. E., Parrington, M., Palmer, P. I., and Lewis, A. C.: Airborne observations of trace gases over boreal Canada during BORTAS: campaign climatology, airmass analysis and enhancement ratios, Atmos. Chem. Phys. Discuss., 13, 14 069–14 114, 2013.

Palmer, P. I., Jacob, D. J., Jones, D. B. A., Heald, C. L., Yantosca, R. M., and Logan, J. A.: Inverting for emissions of carbon monoxide from Asia using aircraft observations over the western Pacific, J. Geophys. Res., 108, 8828, doi:10.1029/2003JD003397, http://doi.wiley.com/10.1029/2003JD003397, 2003.

Palmer, P. I., Suntharalingam, P., Jones, D. B. a., Jacob, D. J., Streets, D. G., Fu, Q., Vay, S. a., and Sachse, G. W.: Using CO 2 :CO correlations to improve inverse analyses of carbon fluxes, J. Geophys. Res., 111, D12 318, doi:10.1029/2005JD006697, http://doi.wiley.com/10.1029/2005JD006697, 2006.

Palmer, P. I., Parrington, M., Lee, J. D., Lewis, a. C., Rickard, a. R., Bernath, P. F., Duck, T. J., Waugh, D. L., Tarasick, D. W., Andrews, S., Aruffo, E., Bailey, L. J., Barrett, E., Bauguitte, S. J.-B., Curry, K. R., Di Carlo, P., Chisholm, L., Dan, L., Forster, G., Franklin, J. E., Gibson, M. D., Griffin, D., Helmig, D., Hopkins, J. R., Hopper, J. T., Jenkin, M. E., Kindred, D., Kliever, J., Le Breton, M., Matthiesen, S., Maurice, M., Moller, S., Moore, D. P., Oram, D. E., O'Shea, S. J., Owen, R. C., Pagniello, C. M. L. S., Pawson, S., Percival, C. J., Pierce, J. R., Punjabi, S., Purvis, R. M., Remedios, J. J., Rotermund, K. M., Sakamoto, K. M., da Silva, a. M., Strawbridge, K. B., Strong, K., Taylor, J., Trigwell, R., Tereszchuk, K. a., Walker, K. a., Weaver, D., Whaley, C., and Young, J. C.: Quantifying the impact of BOReal forest fires on Tropospheric oxidants over the Atlantic using Aircraft and Satellites (BORTAS) experiment: design, execution and science overview, Atmos. Chem. Phys., 13, 6239–6261, doi:10.5194/acp-13-6239-2013, http://www.atmos-chem-phys.net/13/6239/2013/, 2013.

Parrington, M., Palmer, P. I., Henze, D. K., Tarasick, D. W., Hyer, E. J., Owen, R. C., Helmig, D., Clerbaux, C., Bowman, K. W., Deeter, M. N., Barratt, E. M., Coheur, P.-F., Hurtmans, D., Jiang, Z., George, M., and Worden, J. R.: The influence of boreal biomass burning emissions on the distribution of tropospheric ozone over North America and the North Atlantic during 2010, Atmos. Chem. Phys., 12, 2077–2098, doi: 10.5194/acp-12-2077-2012, http://www.atmos-chem-phys.net/12/2077/2012/, 2012.

Parrington, M., Palmer, P. I., Lewis, a. C., Lee, J. D., Rickard, a. R., Di Carlo, P., Taylor, J. W., Hopkins, J. R., Punjabi, S., Oram, D. E., Forster, G., Aruffo, E., Moller, S. J., Bauguitte, S. J.-B., Allan, J. D., Coe, H., and Leigh, R. J.: Ozone photochemistry in boreal biomass burning plumes, Atmos. Chem. Phys. Discuss., 13, 1795–1853, doi:10.5194/acpd-13-1795-2013, http://www.atmos-chem-phys-discuss.net/13/1795/2013/, 2013.

Parrish, D. D., Stohl, A., Forster, C., Atlas, E. L., Blake, D. R., Goldan, P. D., Kuster, W. C., and de Gouw, J. a.: Effects of mixing on evolution of hydrocarbon ratios in the troposphere, J. Geophys. Res., 112, D10S34, doi:10.1029/2006JD007583, http://doi.wiley.com/10.1029/2006JD007583, 2007.

Real, E., Law, K. S., Weinzierl, B., Fiebig, M., Petzold, a., Wild, O., Methven, J., Arnold, S., Stohl, a., Huntrieser, H., Roiger, a., Schlager, H., Stewart, D., Avery, M., Sachse, G., Browell, E., Ferrare, R., and Blake, D.: Processes influencing ozone levels in Alaskan forest fire plumes during long-range transport over the North Atlantic, J. Geophys. Res., 112, D10S41, doi:10.1029/2006JD007576, http://doi.wiley.com/10.1029/2006JD007576, 2007.

Reid, J. S., Hyer, E. J., Prins, E. M., Westphal, D. L., Zhang, J., Wang, J., Christopher, S. a., Curtis, C. a., Schmidt, C. C., Eleuterio, D. P., Richardson, K. a., and Hoffman, J. P.: Global Monitoring and Forecasting of Biomass-Burning Smoke: Description of and Lessons From the Fire Locating and Modeling of Burning Emissions (FLAMBE) Program, IEEE J. Sel. Top. Appl. Earth Obs. Remote Sens., 2, 144–162, doi:10.1109/JSTARS.2009.2027443, http://ieeexplore.ieee.org/lpdocs/epic03/wrapper.htm?arnumber=5208306, 2009.

Spivakovsky, C. M., Logan, J. A., Montzka, S. A., Balkanski, Y. J., Foreman-Fowler, M., Jones, D. B. A., Horowitz, L. W., Fusco, A. C., Brenninkmeijer, C. A. M., Prather, M. J., Wofsy, S. C., and McElroy, M. B.: Three-dimensional climatological distribution of tropospheric OH: Update and evaluation, Journal of Geophysical Research: Atmospheres, 105, 8931–8980, doi:10.1029/1999JD901006, http://dx.doi.org/10.1029/1999JD901006, 2000.

Taylor, J. W., Allan, J. D., Allen, G., Coe, H., Williams, P. I., Flynn, M. J., Le Breton, M., Muller, J. B. A., Percival, C. J., Oram, D., Forster, G., Lee, J. D., Rickard, A. R., and Palmer, P. I.: Size-dependent wet removal of black carbon in Canadian biomass burning plumes, Atmospheric Chemistry and Physics Discussions, 14, 19 469–19 513, doi:10.5194/acpd-14-19469-2014, http://www.atmos-chem-phys-discuss.net/14/19469/2014/, 2014.

Tereszchuk, K. A., Moore, D. P., Harrison, J. J., Boone, C. D., Park, M., Remedios, J. J., Randel, W. J., and Bernath, P. F.: Observations of peroxyacetyl nitrate (PAN) in the upper troposphere by the Atmospheric Chemistry Experiment-Fourier Transform Spectrometer (ACE-FTS), Atmos. Chem. Phys., 13, 5601–5613, 2013.

Yokelson, R. J., Andreae, M. O., and Akagi, S. K.: Pitfalls with the use of enhancement ratios or normalized excess mixing ratios measured in plumes to characterize pollution sources and aging, Atmospheric Measurement Techniques, 6, 2155–2158, doi:10.5194/amt-6-2155-2013, 2013.

Table 1. Contribution of CO from geographical sources averaged over all BORTAS-B flights, lumping all other contributions <2 ppb into "Other". Background refers to any residual CO before the beginning of the BORTAS-B period.

Tracer Source	Mean (ppb)	Std Dev (ppb)
NE USA and Canada Biomass Burning	55.4	134.6
East Asian Fossil Fuel	11.9	3.4
North East American Fossil Fuel	7.9	15.4
NW USA and Canada Biomass Burning	6.2	4.5
North West American Fossil Fuel	3.4	2.2
Mid Siberia Biomass Burning	2.0	0.7
Other	7.9	4.2
Methane & NMVOCS	45.5	12.4
Background	10.7	2.3

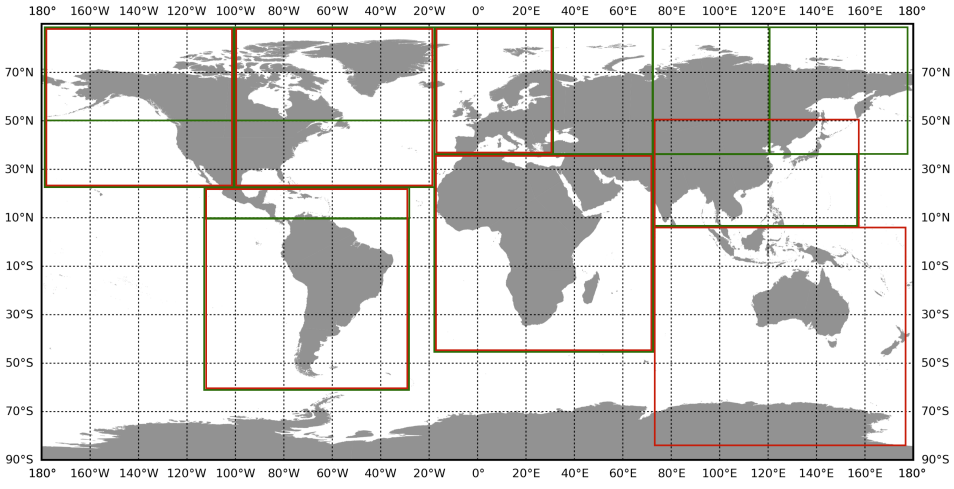

Fig. 1. Source regions for the tagged CO simulation. Regions outlined in red denote fossil fuel tagged tracers and regions outlined in green refer to biomass burning tagged tracers.

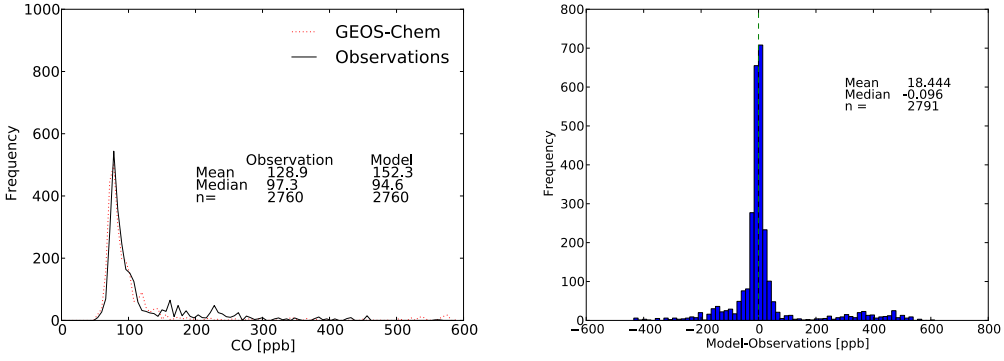

Fig. 2. Statistical comparison of model and observed CO from BORTAS-B. The observations have been averaged over the $2^\circ \times 2.5^\circ$ model grid. Left panel shows the frequency distributions and the right panel show the frequency distribution of the model minus observed CO residuals. Mean and median values are shown inset of each panel.

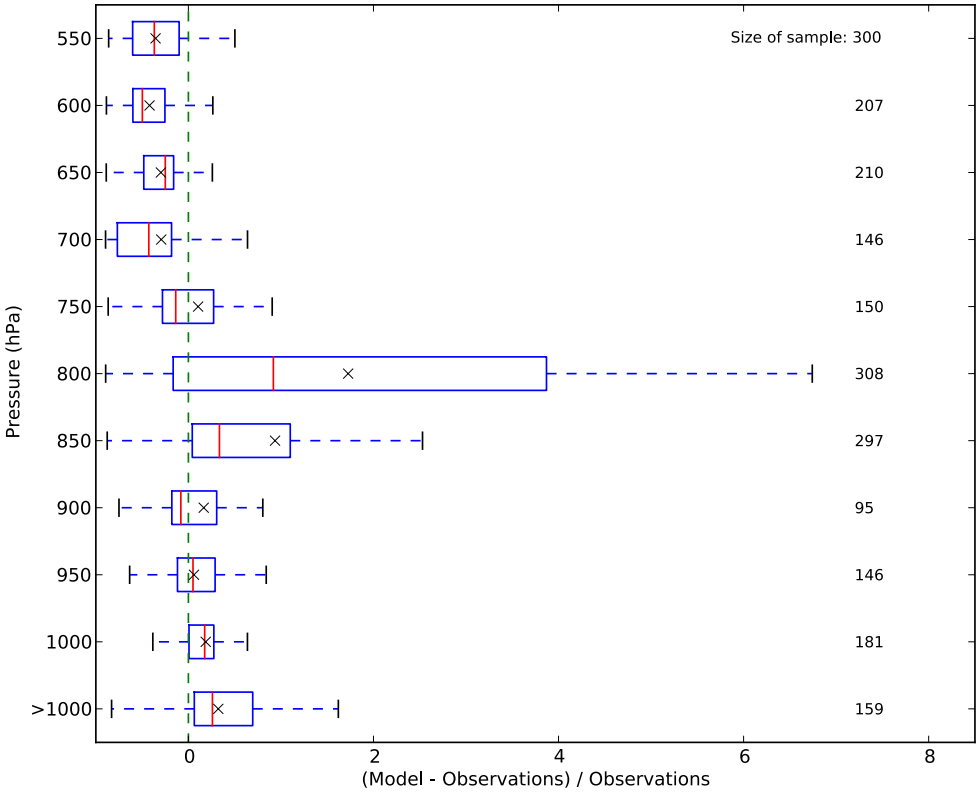

Fig. 3. Relative model error in the GEOS-Chem simulation of CO during BORTAS-B as a function of altitude described by the box and whiskers approach. The red line and grey cross denotes the median and mean values, respectively.

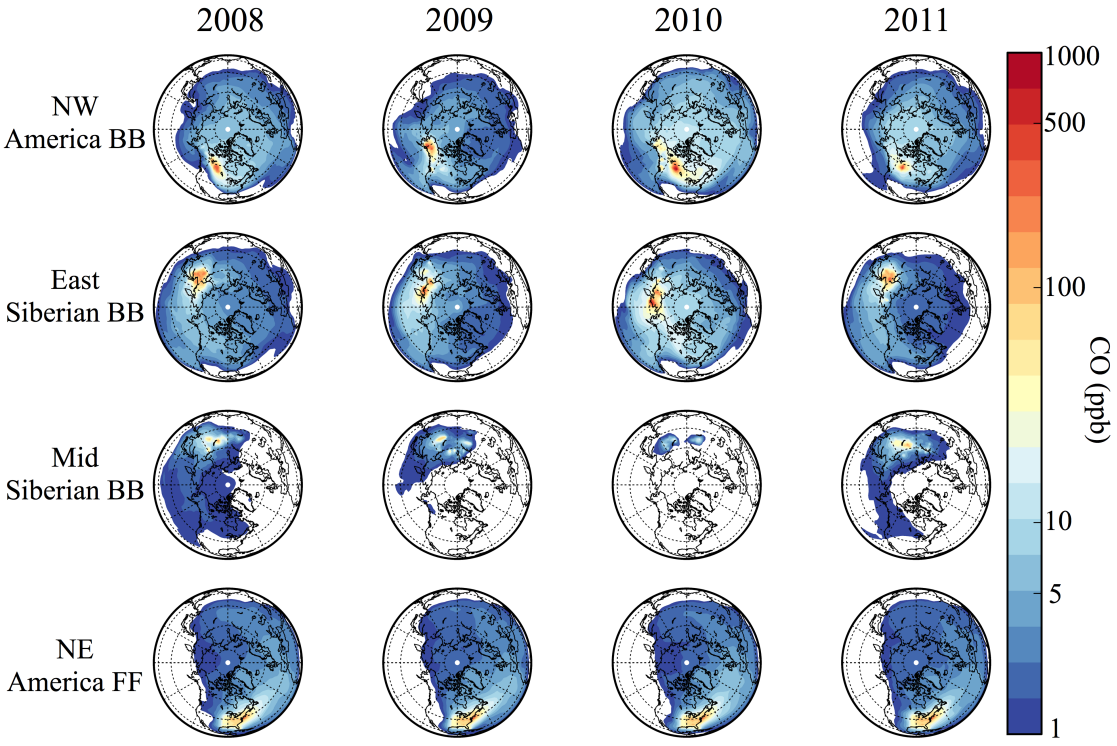

Fig. 4. Mean June-August GEOS-Chem model surface CO concentrations (ppb) from the four largest sources over the northern hemisphere for 2008–2011. Individual contributions (Figure 1) are from NW North America biomass burning emissions (first row), NE North America fossil fuel (second row), East Siberia biomass burning (third row), and mid-Siberia biomass burning (bottom row).

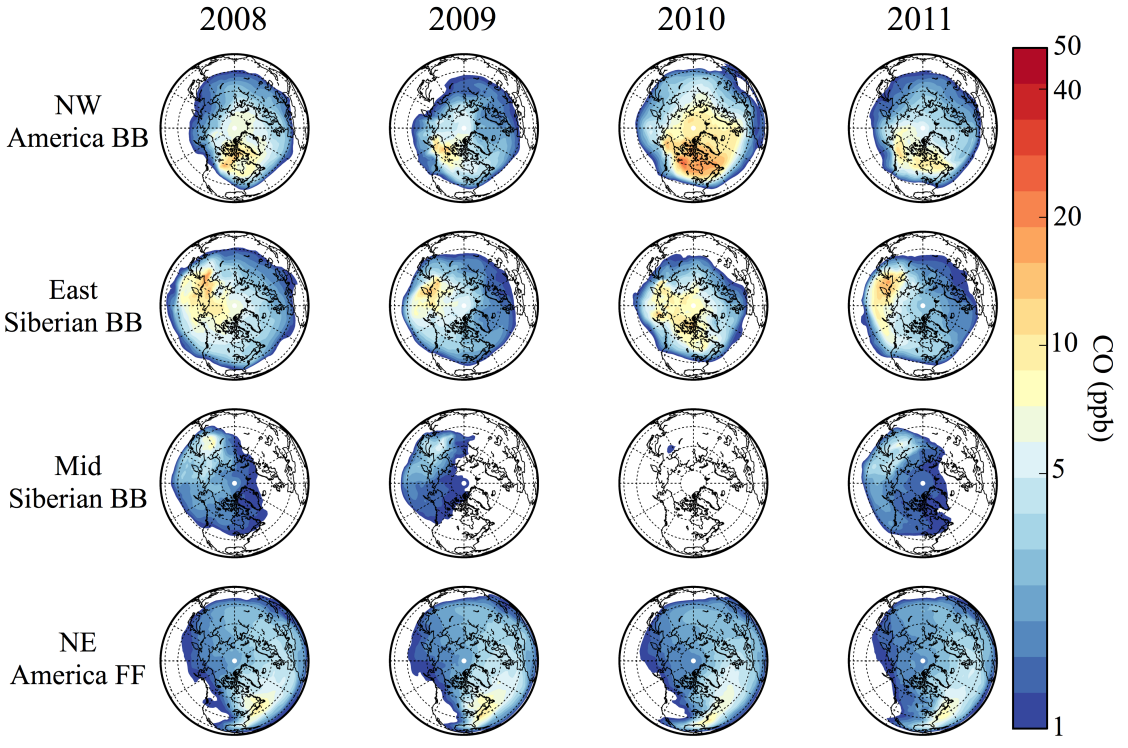

Fig. 5. Same as Figure 4 but at 4 km altitude. Note the different upper limit to the colour bar.

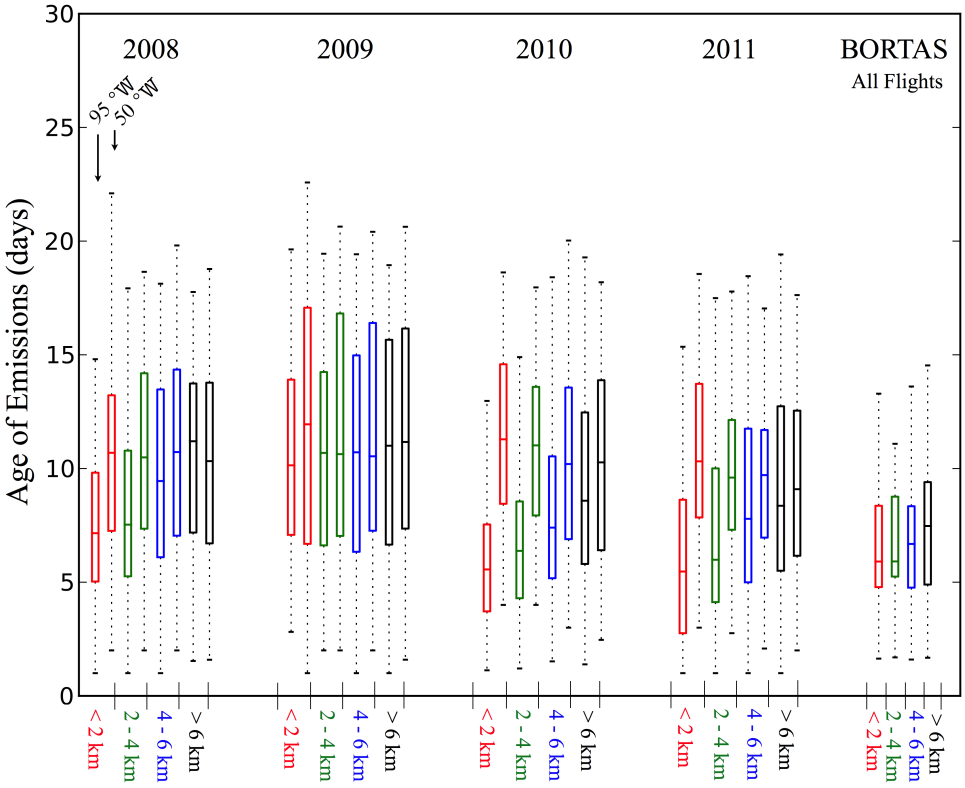

Fig. 6. Box and whiskers plot showing the mean age of emissions for different altitudes (<2 km, 2–4 km, 4–6 km, and >6 km) at the longitudinal boundaries of the BORTAS-B domain (45°N–60° N, 95°W–50°W) during July 2008, 2009, 2010, 2011, and for the model sampled along the BORTAS-B flights. Within the box, the upper, middle, and lower horizontal bars denote the first quartile, the median, and the third quartile. The full range of data is shown by the whiskers.

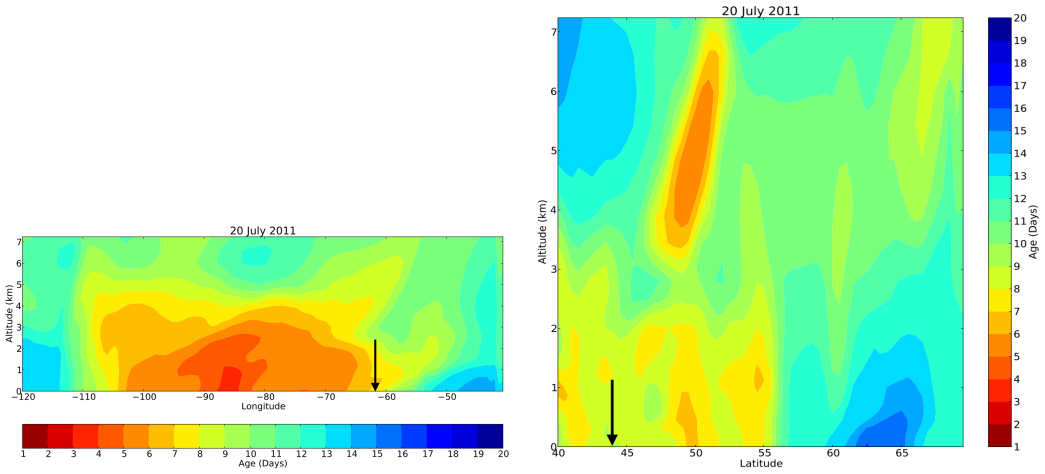

Fig. 7. Age of emissions on 20th July 2011 (left) from 120°–40°W and 0–7 km, averaged over 45°–55°N; and (right) 40°–70°N and 0–7 km at 63°W, the same longitude as the Dalhousie University, Halifax, NS surface measurements (Palmer et al., 2013). Location of Dalhousie University is shown by the black arrow.

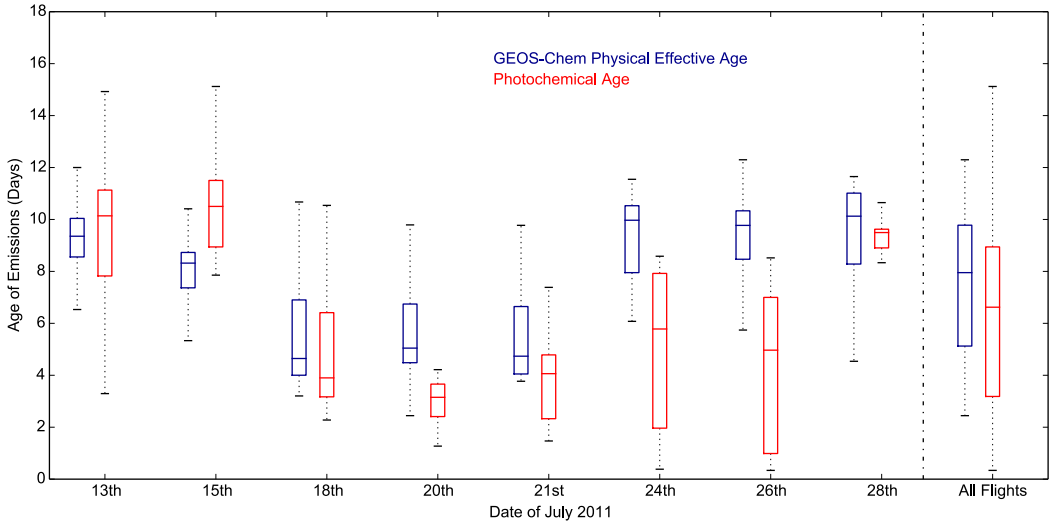

Fig. 8. Box and whiskers plot of the age of air observed during individual BORTAS-B aircraft flights using photochemical age using BORTAS-B data (red) and effective age $\bar{A}$ using the GEOS-Chem model (blue). The box and whiskers plot for all flights are shown on the last two right columns. Within the box, the upper, middle, and lower horizontal bars denote the first quartile, the median, and the third quartile. The full range of data is shown by the whiskers.

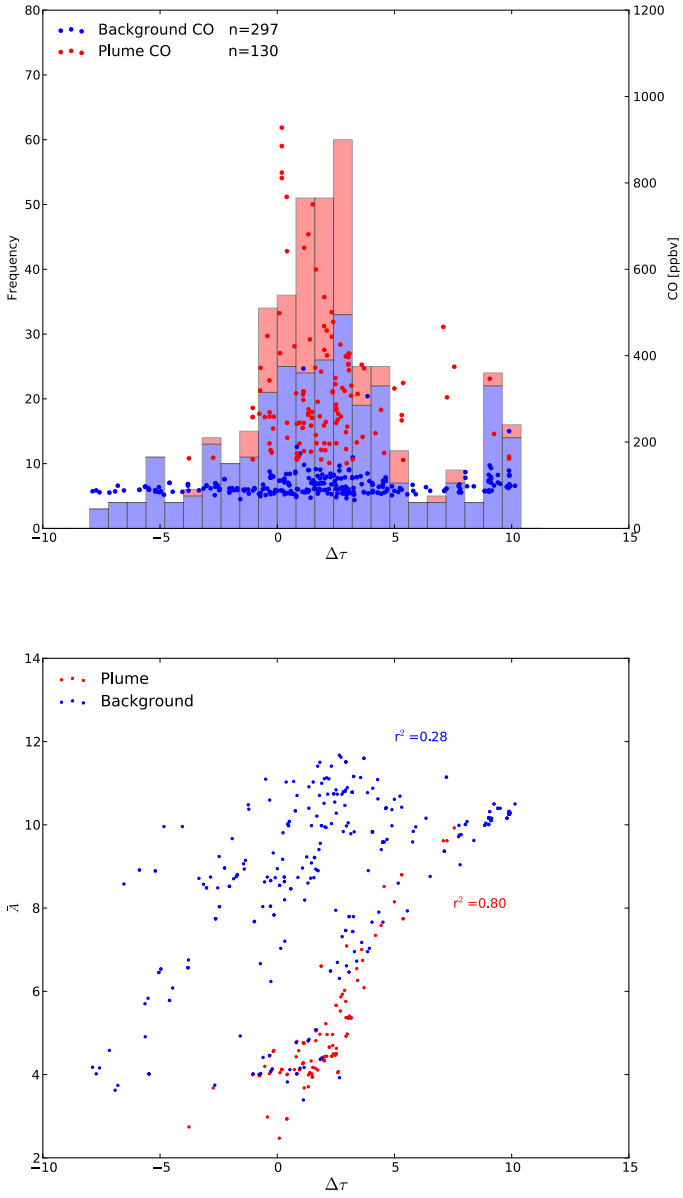

Fig. 9. Top Panel: Frequency of effective age $\bar{A}$ minus photochemical age (days, left axis) and CO concentration (ppb, right axis). The number of measurements n for each classification are shown inset. Bottom Panel: Scatterplot of $\Delta\tau$ and $\bar{A}$. Red dots denote CO concentrations within a plume (CH_3CN> 150 ppt) and the blue dots denote CO concentrations outwith a plume.